Journal of Hazardous Materials 166 (2009) 469–477

Contents lists available at ScienceDirect

Journal of Hazardous Materials

journal homepage: www.elsevier.com/locate/jhazmat

Diesel oil pool fire characteristic under natural ventilation conditions in tunnels with roof openings

Yanfu Wang [a], Juncheng Jiang [a,*,1], Dezhi Zhu [b]

[a] Nanjing University of Technology, Jiangsu Key Laboratory of Urban and Industrial Safety, Nanjing 210009, China
[b] Nanjing General Fire Brigade, Nanjing 210009, China

ARTICLE INFO

Article history:
Received 29 August 2008
Received in revised form
14 November 2008
Accepted 15 November 2008
Available online 27 November 2008

Keywords:
Tunnel fire
Full-scale experiment
Field simulation
Smoke

ABSTRACT

In order to research the fire characteristic under natural ventilation conditions in tunnels with roof openings, full-scale experiment of tunnel fire is designed and conducted. All the experimental data presented in this paper can be further applied for validation of numerical simulation models and reduced-scale experimental results. The physical model of tunnel with roof openings and the mathematical model of tunnel fire are presented in this paper. The tunnel fire under the same conditions as experiment is simulated using CFD software. From the results, it can be seen that most smoke is discharged directly off the tunnel through roof openings, so roof openings are favorable for exhausting smoke. But along with the decrease of smoke temperatures, some smoke may backflow and mix with the smoke-free layer below, which leads to fall in visibility and is unfavorable for personnel evacuation. So it is necessary to research more efficient ways for improving the smoke removal efficiency, such as early fire detection systems, adequate warning signs and setting tunnel cap.

1. Introduction

Tunnel fire is a hot concern around the world due to big fire disasters occurring in road or railway tunnels in recent years. The fires in the Tauern tunnel in Austria, the Mont Blanc tunnel joining France to Italy and the Channel tunnel joining the UK to France have highlighted the issue and shown the devastating effect of such fires, in terms of loss of life, damage to facilities and destruction of vehicles. The environment in the tunnel will be polluted by smoke particle and poisonous gases, such as carbon monoxide, produced by the fire. The smoke particles decrease the visibility range and induce that the evacuee cannot find their way out. Also, the toxic gases may directly harm and kill the evacuee. So fire protection and ventilation are now seen as the key elements in tunnel design and smoke characteristic in tunnel fires has been one of the main research topics [1].

Methods for analysis of smoke characteristic in tunnel fires are full-scale experiment, reduced-scale experiment and numerical simulation. Because a full-scale experiment can be assumed as a real situation, it provides the most useful data among these methods. However, it is high in cost, time-consuming and has a risk of fire. A reduced-scale experiment can have a flow characteristic like a real situation by application of a scaling law. But careful attention must be paid to the application of a scaling factor between the prototype and model otherwise reduced-scale experiment may fail to revert to a real situation. Numerical simulation can be analyzed repeatedly under various conditions. But it contains many assumptions. If experimental data are not provided for comparison, the numerical simulation results cannot be validated [2].

Apart from saving money in new tunnels with roof openings, natural ventilation could also be useful in the tunnels where installing a high-capacity mechanical ventilation system is difficult, especially for relatively short, shallow tunnels such as those found in urban areas. This tunnel is the first urban road tunnel to adopt natural ventilation with roof openings in China. Whether it can effectively exhaust smoke in real fires is still unknown. So it is necessary to validate its reliability by experiments. Although a number of fire experiments have been carried out in tunnels over the past few decades, those experiments were generally designed to investigate smoke control under forced ventilation conditions [3–4], rather than to study the smoke properties under natural ventilation conditions. One objective of this paper is to research the smoke characteristic under natural ventilation conditions in tunnel fire with roof openings by full-scale experiment. The other purpose is to assess the performance of CFD models comparing with experimental data under a difficult condition where roof openings affect the movement of smoke.

* Corresponding author. Tel.: +86 13951814367; fax: +86 2583587411.
E-mail address: j_c_jiang@163.com (J. Jiang).
[1] This work was supported by National Natural Science Foundation of China under Grant No. 50206009.

0304-3894/$ – see front matter © 2008 Elsevier B.V. All rights reserved.
doi:10.1016/j.jhazmat.2008.11.056

Fig. 1. Interior photograph of tunnel configurations.

2. Description of fire scenario

2.1. Tunnel configuration

The tunnel is two-tube, one-directional on three lanes. Its northbound tunnel (experimental domain) is 12.35 m wide, 5.75 m high and 1410 m long. Roof openings distribute symmetrically on the mid-board between the two tubes and the cross-section of one roof opening is 3.0 m × 2.6 m. Four openings constitute one group with 0.8 m interval between two openings and between two groups the space is 8.8 m wide (see Figs. 1 and 2). Upon every opening, there is a beam, which is 0.8 m wide and 2 m high, near the top of tunnel. The velocity of natural wind outside the tunnel is 2–3 m/s. In the tunnel, the velocity of natural wind maintains 0.4–1.2 m/s and the average velocity is 0.95 m/s or so.

2.2. Heat release rate

This tunnel prohibits vehicles with dangerous chemicals or heavy goods from passing by. So the self-ignition of medium cars (about 5 MW) is the probable danger in the tunnel fires. Diesel oil added small amounts of gasoline (5–10%) were used as fuel [5]. Firstly, the pool fire (about 7.5 MW) was calibrated by oxygen consumption way in the lab ahead of full-scale experiments. The heat release rate of the pool fire was calculated from mass loss rates of the fuel, with the combustion heat to be 42,000 kJ/kg. The combustion efficiencies of the pool fire were measured and deduced in the large-space lab by the oxygen consumption way, combing with measurements of mass flow rate [6–8]. And then it is assumed that the same heat release rate is obtained with the same diesel oil pool in the tunnel configuration.

2.3. Fire source location

In many real fires of road tunnel, the fire originates near the sidewall [9], so the fire source is located at 3 m away from the exterior wall in this experiment. This tunnel adopts natural ventilation with roof openings, so the worst location for exhausting smoke is in the middle of the longest section without roof openings, at which the fire source location is set to study the worst case. The sketch map of fire source location is shown in Fig. 3. The plane layout of measurement system is shown in Fig. 4

2.4. Experimental results and analysis

After ignition, hot smoke rises driven by thermal buoyant force and entrains ambient cold air, forming smoke plume. Smoke plume impinges on the tunnel ceiling and then spreads upstream and downstream at the same time. In the early stage, an upper quiescent buoyant smoke layer is formed with a cold smoke-free layer below. After longer longitudinal propagation, the buoyancy becomes weaker with the decrease of temperature difference and then the head of hot current falls down and mixes with cooler air. The smoke front will halt when the buoyancy equals the applied force of longitudinal natural wind. When the new hot smoke is supplied from the fire source, the smoke front will continue to advance and then wander again under the effect of longitudinal natural wind. Arriving at the roof openings most smoke flow through the roof openings in the early stage, but along with the decrease of thermal pressure, smoke may flow back and mix with smoke-free air. When the new hot smoke from the fire source is supplied and thermal pressure is larger than wind pressure, smoke flows outside the tunnel through the roof openings again [10]. The detailed information of temperature field, smoke propagation and smoke sedimentation is described in the first test of Ref. [10].

3. Numerical simulation of tunnel fire

The cutting-edge technology for representing the complex phenomenon of fire and smoke propagation in the simulation space is computational fluid dynamics (CFD). This methodology solves the fundamental equations describing fluid flow: the time-dependent Navier–Stokes equations and the issues surrounding the heat transfer phenomena associated with fire. In addition, it is necessary

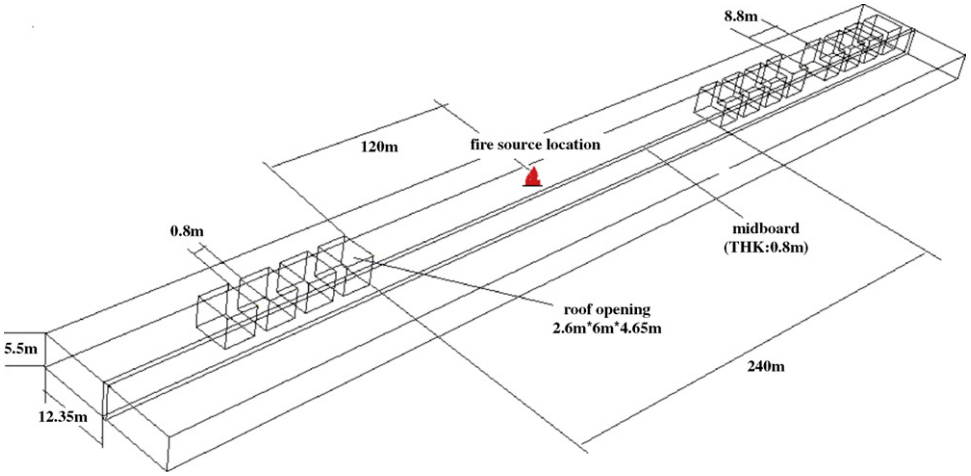

Fig. 2. Schematic illustration of tunnel configurations.

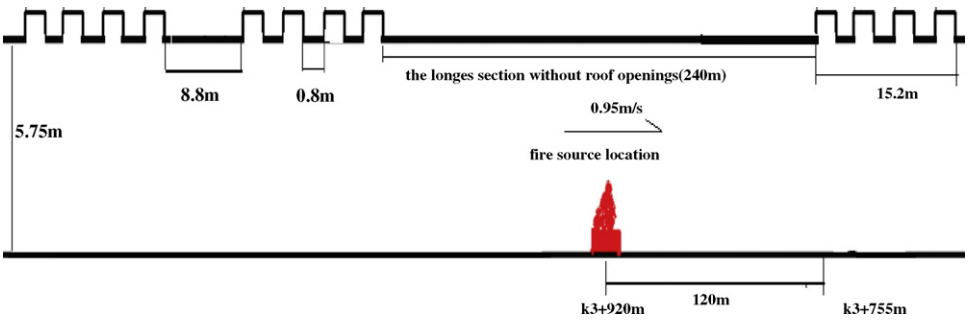

Fig. 3. Disposal map of fire source.

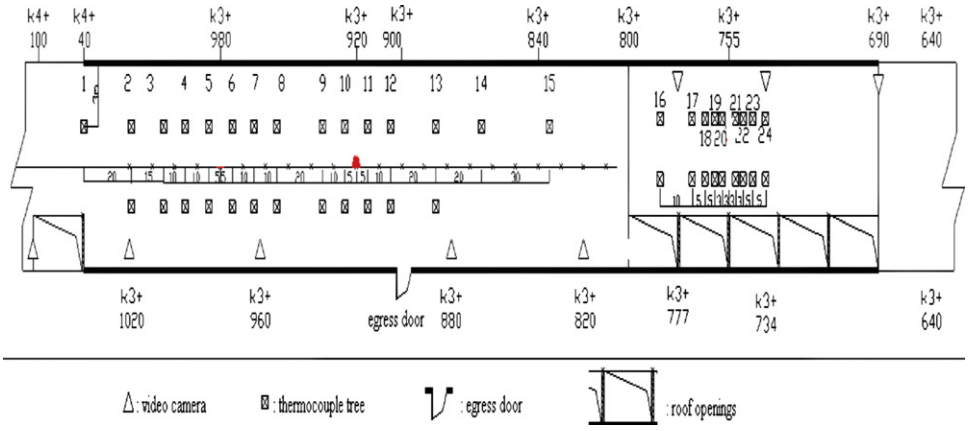

Fig. 4. Plane layout of measurement system.

to couple the combustion chemistry of the processes with the equations describing the transport of species [11]. In this paper, numerical simulation is carried out to analyze the smoke characteristics in tunnel fires with roof openings using the FLUENT software, a commercial CFD code [12]. The governing equations are solved using the finite-volume method on a staggered grid system. To account for the radiant heat in tunnel fires, the Rosseland model is incorporated into the turbulence k–ε model together.

3.1. Physical model

The tunnel fire under the similar conditions as experiments is simulated with FLUENT software: the size of physical model is the same as the tunnel entity structure's, the fire source location is set in the middle of the longest section without roof openings and the heat release rate of the pool fire is 7.5 MW. What conditions are not matched between the experiment and CFD is the adiabatic boundary conditions are assumed on all the solid walls and the fire source is simplified as the source of heat and smoke in simulation. In order to reduce the number of grid points and save computation time, the numerical simulation of tunnel fire is carried out in half domain of the tunnel with the dimension of 230 m × 5.75 m × 12.35 m (length × height × width) due to the symmetric structure of the tunnel, which is shown in Fig. 5. The grid-independent tests have been performed through a series of computations by using different grid numbers, including 54,862, 109,724, 475,264, 694,532 and 1,078,453. Fig. 6 shows the grid test results by using the different grid systems. From the figure, it can be seen that drag coefficient (DC) of wind is almost constant value and the difference is smaller than one percent when the grid count is lager than 475,264. Accordingly, the 475,264-grid system is selected in present simulations. The layout of the computational grid system is shown in Fig. 7.

3.2. Combustion model

Three representative combustion models for computational fluid dynamics are the volumetric heat source (VHS) model, the eddy break-up model and the presumed probability density function (prePDF) model [13]. The volumetric heat source model is the simplest model for combustion. The fire source is modeled as a volumetric heat source, which is patched into the computational domain. For the case of tunnel fire, a mass source is also patched

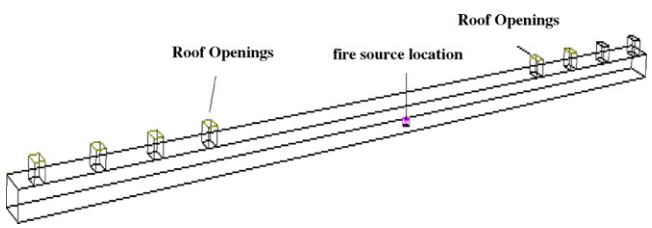

Fig. 5. The physical model of tunnel.

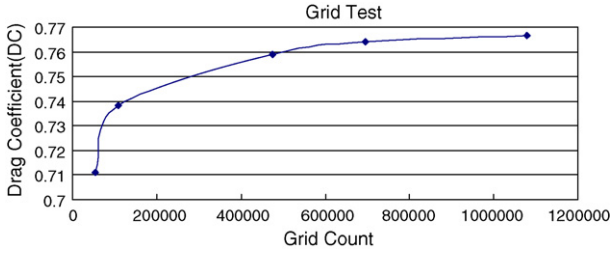

Fig. 6. Grid test results.

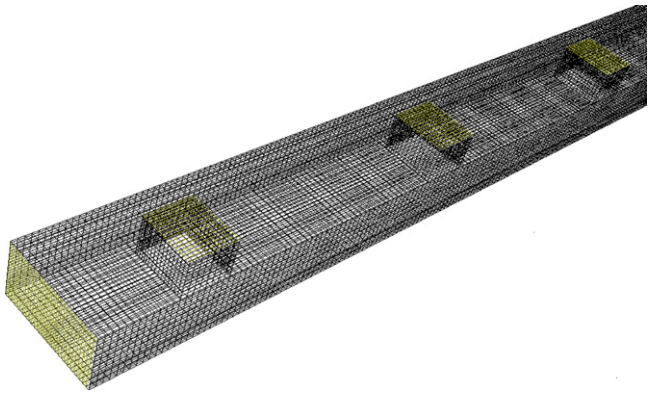

Fig. 7. Part computational grid.

to account the smoke entering to the tunnel from a diesel oil pool. VHS model is chosen as combustion model in this paper. The tunnel fire is considered as the source of heat and smoke. As found from the fuel analysis of combustion, a fire of heat release rate 7.5 MW is accompanied by smoke generation rate 0.78125 kg/s. There is enough oxygen in tunnels with roof openings, so the most combustion product is carbon dioxide. It is assumed that there is not any chemical reaction during smoke flowing.

3.3. Mathematical model

Heated air movement is the key concern in tunnel fires. The turbulent buoyant flow is governed by the equations expressing the conservation of mass, momentum, concentration and energy [14]. When unsteady-state process is considered, the governing equations can be written in a common format as

$$\frac{\partial}{\partial t}(\rho\phi) + \mathrm{div}(\rho u\phi) = \mathrm{div}(\Gamma \mathrm{grad}\phi) + S_\phi \quad (1)$$

where ϕ denotes common dependent variable, ρ denotes density, u denotes velocity vector, Γ denotes diffusion coefficient, S_ϕ denotes remaining term. Those four left-to-right terms stand for transient term, convection term, diffusion term and source term, respectively. The detailed equations are shown in Table 1.

The fully implicit scheme is implemented with a variable time increment determined by control of the local time truncation error at each time step.

$$\frac{\partial}{\partial t}(\rho\phi) + \mathrm{div}(\rho u\phi) = \mathrm{div}(\Gamma \mathrm{grad}\phi) + S_\phi \quad (2)$$

where $a_P = (a_E + a_W) + (F_e - F_W) + a_P^0 - S_p\Delta V \;\; a_P^0 = \rho\Delta V/\Delta t \;\; a_W$ and a_E are determined by discrete scheme.

The k–ε turbulence model has been used for turbulence closure that implies solving two additional equations, the equation of conservation of turbulent kinetic energy (k) and the corresponding one to its dissipation (ε).To calculate the smoke concentration also the conservation equation of that species had to be solved, considering the system as a binary mixture of air and smoke. FLUENT predicts the local mass fraction of each species, Y_i, through the solution of a convection–diffusion equation for the ith species. This conservation equation takes the following general form: $(\partial/\partial t)(\rho Y_i) + \nabla \cdot (\rho\vec{v}Y_i) = -\nabla \cdot \vec{J}_i + R_i + S_i$. Where R_i is the net rate of production by chemical reaction, $\vec{J}_i$ is the diffusion flux of species i, and S_i is the rate of creation by addition from the dispersed phase plus any user-defined sources. The numerical resolution of the Navier–Stokes equations have been carried out using second order upwind scheme for the convective terms and first order upwind scheme for the diffusion terms. The coupling between equations through the pressure has been solved using the SIMPLEC method.

3.4. Boundary conditions

Ambient temperature is assumed to be 280 K. Pressure-inlet (or velocity-inlet) boundary condition is given in the tunnel entrance and pressure-outlet is given in the tunnel exit. Pressure-inlet boundary condition is assumed on the roof openings. The operating pressure is 101,325 Pa, gauge total pressure is 0 Pa, hydrostatic pressure is defined as $P_s' = P_s - \rho_0 g x$ and direction specification method is normal to boundary. On the solid walls, a non-slip condition, the adiabatic boundary conditions, constant temperature and zero smoke flux are assumed. As the convergence criterion, the sum of the normalized absolute residuals in each control volume for all the other variables to be less than 10^{-3} except 10^{-6} for energy. The maximum iterations per time step is 80 and the computing time requires almost 54 h using Core (TM) 2, 1.6 GHz PC.

3.5. Numerical simulation results

3.5.1. Pressure-inlet boundary condition case

Figs. 8–12 plot the simulation results of the temperature distributions along vertical central plane under the conditions of $V_0 = 0.95$ m/s (V_0: initial mean wind velocity, the wind direction is from left-to-right) and $Q'' = 7.5$ MW (Q'': heat release rate) when pressure-inlet boundary condition is given in the tunnel entrance. From the above figures, It is easy to see that after 40 s, smoke

Table 1
Coupled equations for control of 3D field model for smoke movement.

Equations	ϕ	Γ	S_ϕ
Continuity equation	1	0	0
x-Momentum equation	u	μ	$-\frac{\partial p}{\partial x} + \frac{\partial}{\partial x}\left(\mu\frac{\partial u}{\partial x}\right) + \frac{\partial}{\partial y}\left(\mu\frac{\partial v}{\partial x}\right) + \frac{\partial}{\partial z}\left(\mu\frac{\partial w}{\partial x}\right)$
y-Momentum equation	v	μ	$-\frac{\partial p}{\partial y} + \frac{\partial}{\partial x}\left(\mu\frac{\partial u}{\partial y}\right) + \frac{\partial}{\partial y}\left(\mu\frac{\partial v}{\partial y}\right) + \frac{\partial}{\partial z}\left(\mu\frac{\partial w}{\partial y}\right)$
z-Momentum equation	w	μ	$-\frac{\partial p}{\partial z} + \frac{\partial}{\partial x}\left(\mu\frac{\partial u}{\partial z}\right) + \frac{\partial}{\partial y}\left(\mu\frac{\partial v}{\partial z}\right) + \frac{\partial}{\partial z}\left(\mu\frac{\partial w}{\partial z}\right) - \rho g$
Enthalpy equation	h	$\frac{\mu}{\sigma_h}$	$q_s - q_r$[a]
Composition equation	C_s	$\frac{\mu}{\sigma_c}$	w_s[b]
Turbulent kinetic energy equation	k	$\frac{\mu}{\sigma_k}$	$G - \rho\varepsilon$
Turbulent dissipation rate equation	ε	$\frac{\mu}{\sigma_\varepsilon}$	$\frac{\varepsilon}{k}(C_1 G - C_2\rho\varepsilon)$
$\mu = \mu_l + \mu_T$	$\mu_T = \frac{C_\mu \rho k^2}{\varepsilon}$		$G = G_k + G_b = \mu_T\left(\frac{\partial u_i}{\partial x_j} + \frac{\partial u_j}{\partial x_i}\right)\frac{\partial u_j}{\partial x_i} - \mu_t\frac{g_i}{\rho}\frac{\partial \rho}{\partial x_i}$
$C_u = 0.09$, $C_1 = 1.44$	$C_2 = 1.92$	$\sigma_k = 1.0$	$\sigma_\varepsilon = 1.3$, $\sigma_h = 0.9$, $\sigma_c = 0.9$

[a] q_s stand for combustion heat flux. q_r stand for radiating source terms.
[b] w_s stand for smoke quality.

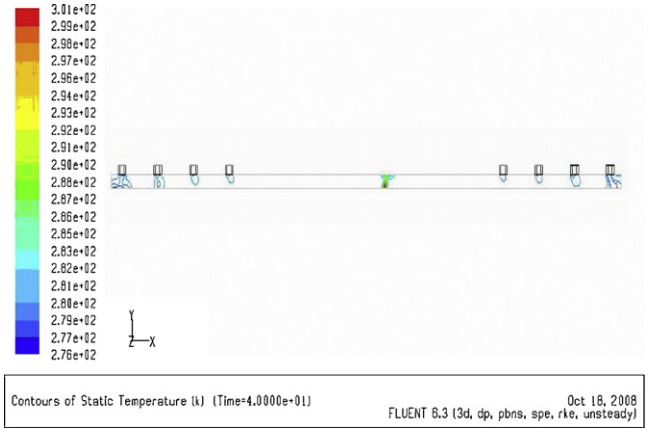

Fig. 8. Smoke temperature of vertical central plane (40 s).

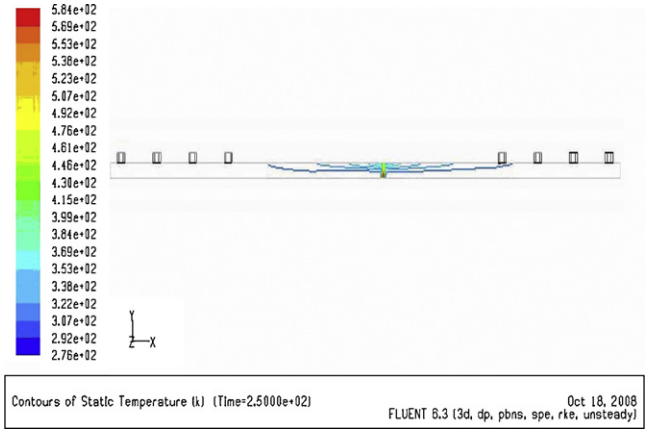

Fig. 9. Smoke temperature of vertical central plane (250 s).

impinges on the tunnel ceiling and there is evident ceiling jet; 250 s after ignition, smoke front arrives at the first opening downstream and some smoke flows outside the tunnel through the first opening; 340 s after ignition, downstream smoke front reaches the second opening, upstream smoke front arrives at the first opening and all smoke flow outside through the first opening leaving the front section free of smoke; 380 s after ignition downstream smoke front arrives at the third opening; 440 s after ignition smoke sedimentation becomes severe and smoke basically fills with the whole section without openings, which is a little different from

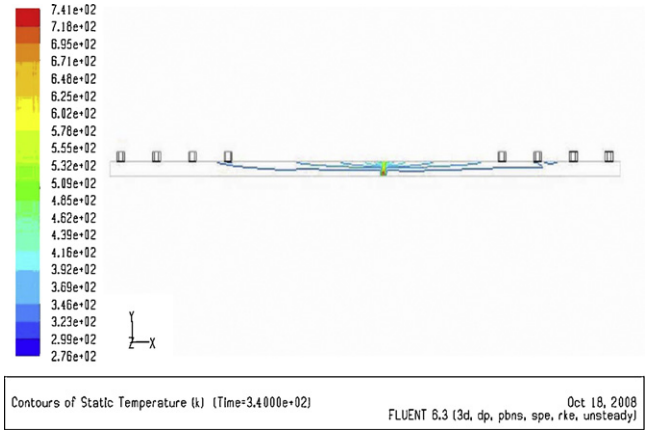

Fig. 10. Smoke temperature of vertical central plane (340 s).

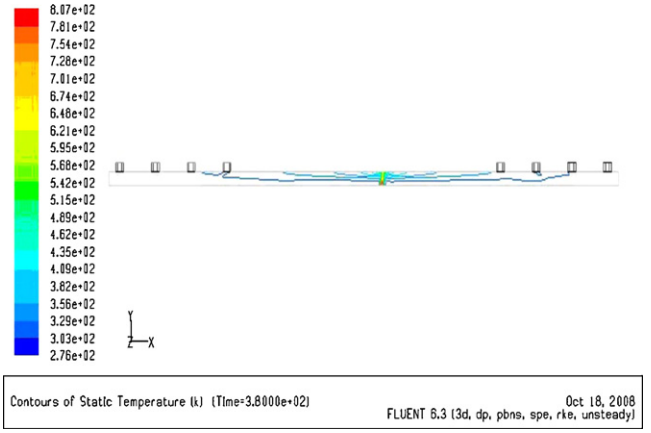

Fig. 11. Smoke temperature of vertical central plane (380 s).

the experimental phenomenon. From Figs. 8–12 we can also see that smoke temperature is higher in the vicinity of the fire and the maximum temperature is 854 K after 440 s. We can also see that longitudinal propagation of downstream smoke is quicker than the upstream one, which is more obvious near the fire source and there is enough time for evacuating. Hence the roof openings are very useful for restraining the longitudinal propagation of smoke under this condition.

The smoke temperature vertical distribution on cross-section of fire source location, 5 m upstream, 5 m downstream, 15 m upstream and 15 m downstream are plotted in Figs. 13–19. It can be seen that smoke temperature near fire source is quite high and the maximum temperature is 850 K after 420 s. The maximum temperature under the ceiling is between 500 and 600 k, which is higher than experimental data. Smoke temperature lowers rapidly with the increase of the longitudinal distance from fire source. From the above figures, we can also see that there is evident smoke stratification; smoke temperature of different layer is evidently different from each other; high-temperature smoke layer does not fall to 1.8 m high before 360 s, which does not threaten personnel safety as shown in Fig. 19, which leads to fall in visibility and difficulty in breathing. In the vicinity of the fire, the smoke layer near wall region is lower than that of tunnel midsection but gradually become same high along with the increase of the longitudinal distance from fire source. As hot smoke moves outward under the ceiling, smoke transfers energy by conduction to the relatively cool adjacent ceiling surface and by convection to the entrained air. It is retarded by friction forces from the ceiling surface above and turbulent momentum

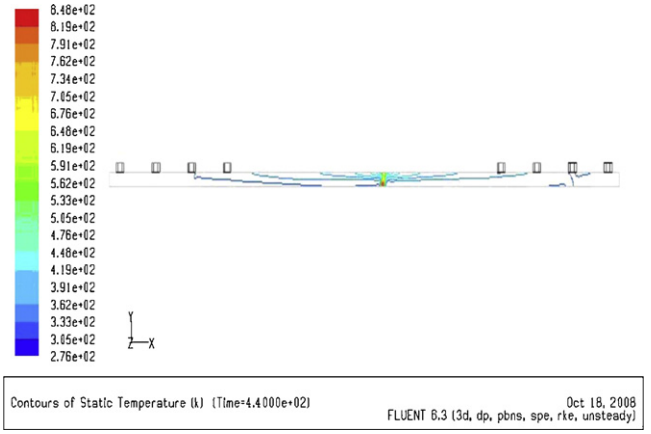

Fig. 12. Smoke temperature of vertical central plane (440 s).

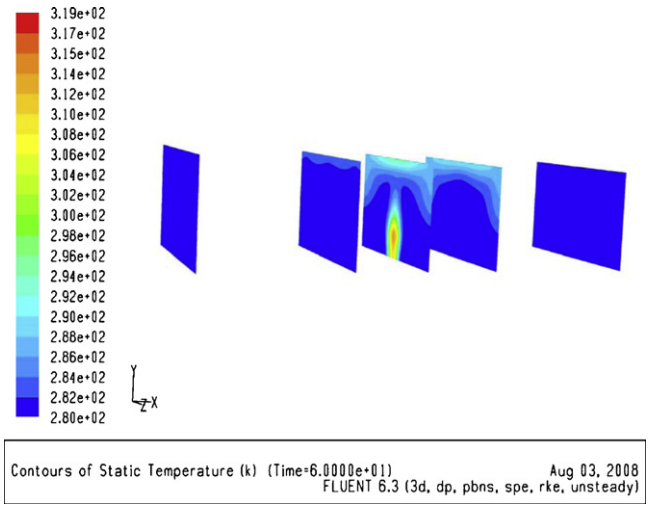

Fig. 13. Smoke temperature of cross-section (60 s).

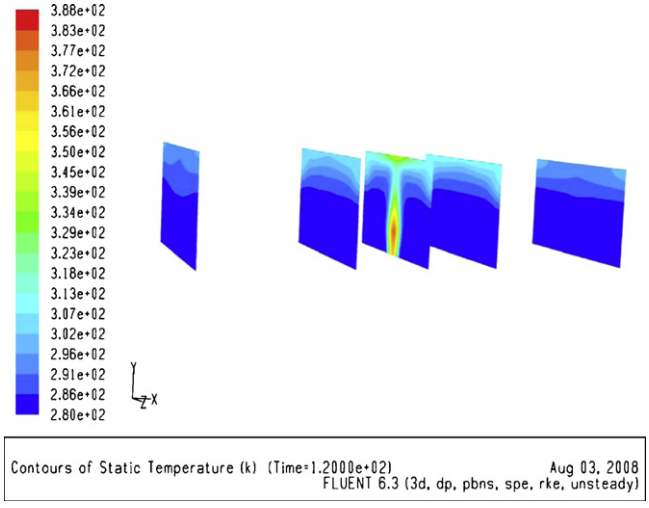

Fig. 14. Smoke temperature of cross-section (120 s).

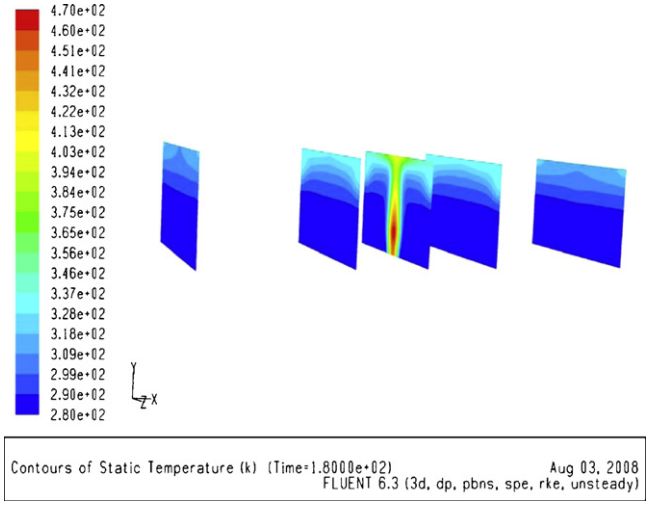

Fig. 15. Smoke temperature of cross-section (180 s).

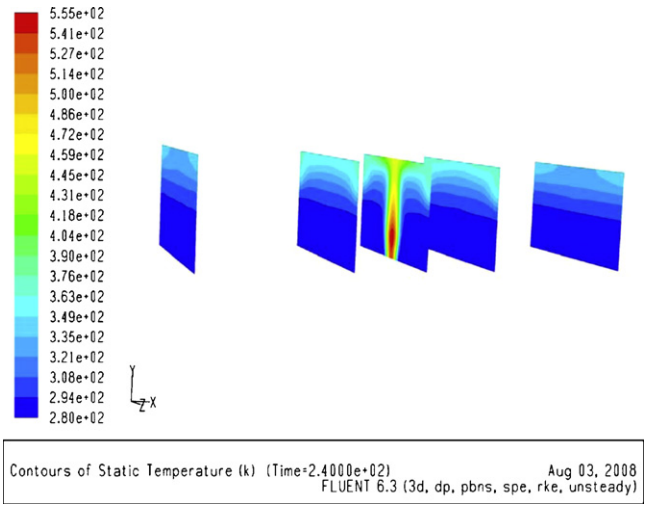

Fig. 16. Smoke temperature of cross-section (240 s).

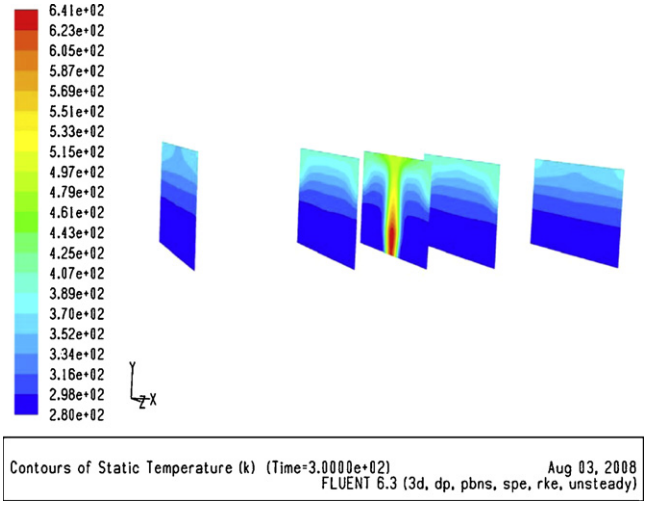

Fig. 17. Smoke temperature of cross-section (300 s).

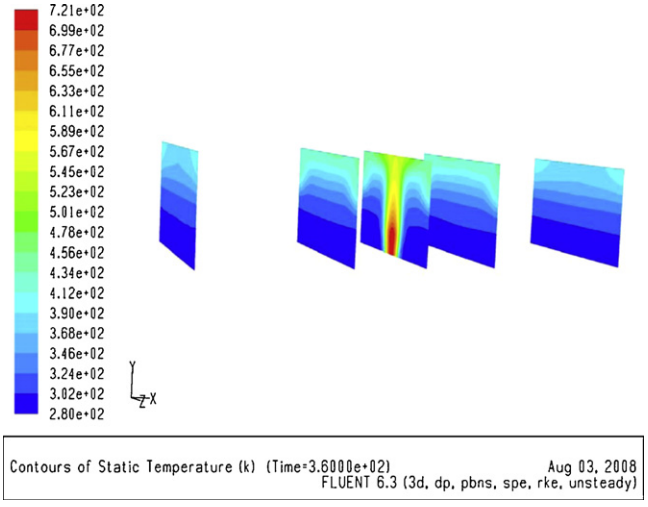

Fig. 18. Smoke temperature of cross-section (360 s).

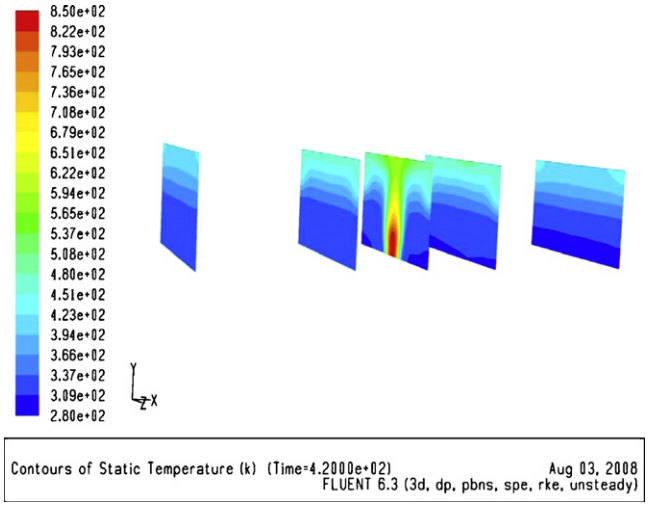

Fig. 19. Smoke temperature of cross-section (420 s).

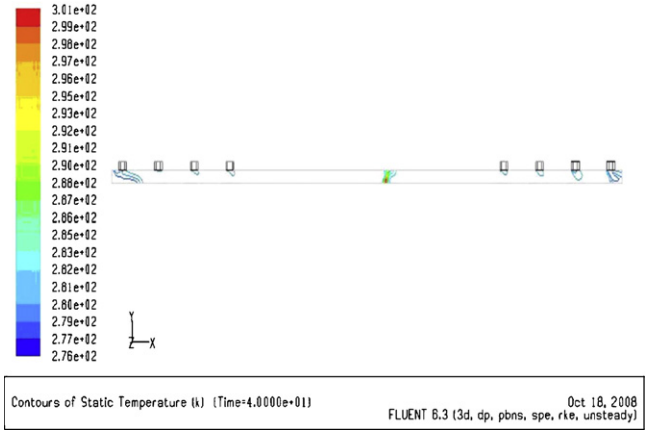

Fig. 20. Smoke temperature of vertical central plane (40 s).

transfer to the entrained air from below. Owing to these effects smoke layer thickness grows thicker as time elapses.

3.5.2. *Velocity-inlet boundary condition case*

Figs. 20–24 plots the simulation results of the temperature distributions along vertical central plane when velocity-inlet boundary condition is given in the tunnel entrance while the other conditions unchanged. From above figures, it can be seen that simulation results are almost identical with pressure-inlet boundary condition case, whose temperature, smoke longitudinal propagation and smoke sedimentation are similar to each other; the smoke back flow is not affected by the way of imposing boundary conditions.

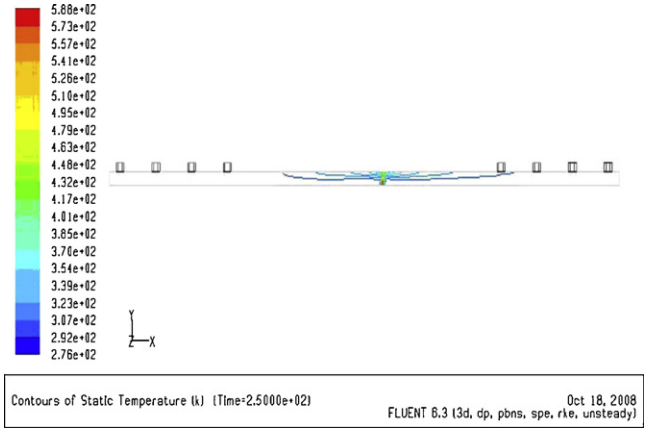

Fig. 21. Smoke temperature of vertical central plane (250 s).

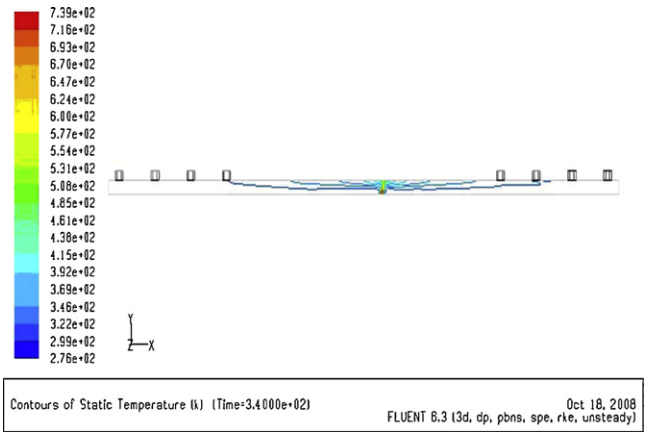

Fig. 22. Smoke temperature of vertical central plane (340 s).

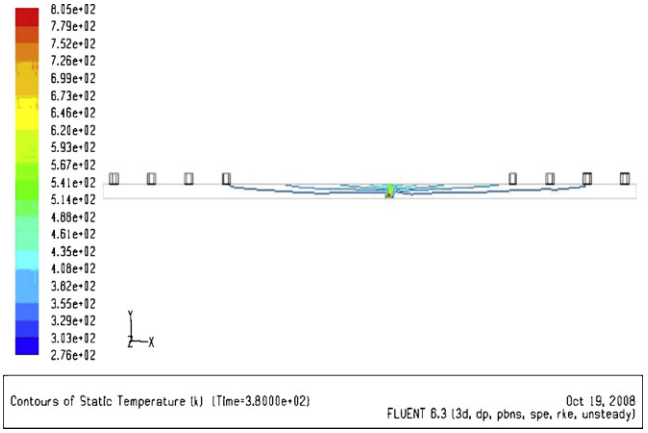

Fig. 23. Smoke temperature of vertical central plane (380 s).

4. Comparisons between numerical simulation results and experimental data

Before a CFD code can be proposed as an alternate method for the prediction of tunnel fire, it has to be validated with proper experimental data. In order to checkout FLUENT whether can be used for simulating tunnel fire with roof openings, the following compar-

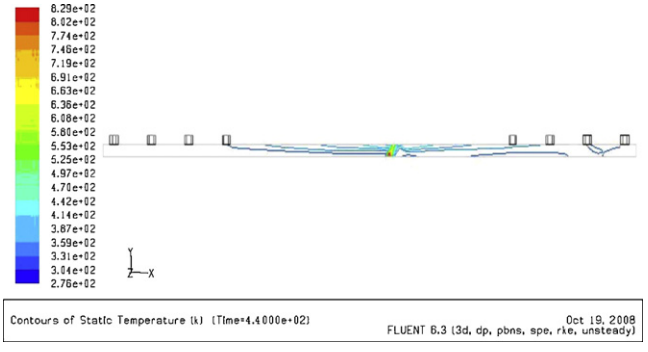

Fig. 24. Smoke temperature of vertical central plane (440 s).

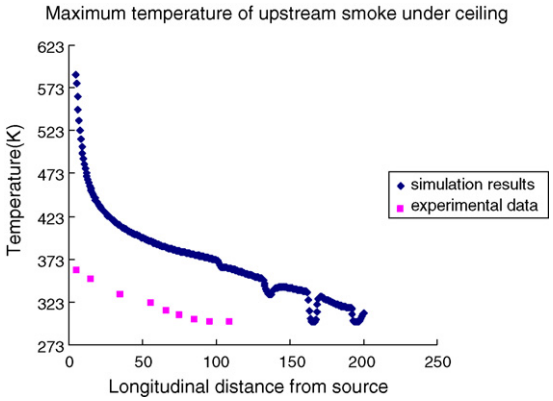

Fig. 25. Maximum temperature under ceiling of different upstream distance from fire source.

isons between simulation results and experimental data are carried out.

4.1. Comparison of the maximum temperature under the ceiling

Comparing the simulative maximum temperature under the ceiling with experimental data is shown in Figs. 25 and 26. It can be seen that variation trend of simulation results and experimental data is identical: the maximum temperature (at any time) under the ceiling lowers continuously with the increase of the longitudinal distance due to the heat lost to the cold ceiling and entrainment cold air, which is in a safe range for tunnel structure. Temperatures near the fire source are much higher than those locations far away from the fire source. In the vicinity of fire source, smoke remains sufficiently hot. This is because the heat supplied to the smoke from the fire source is much larger than that carried away by convection with cold air and conduction from the smoke layer to the tunnel boundary. The maximum temperature measured in the experiment is 373 K, while the simulative maximum temperature under the ceiling is 600 K, which is because the adiabatic boundary conditions are assumed on all the solid walls in simulation. In the vicinity of the fire source, simulative temperature is quite high. This is because the fire source is simplified as the source of heat and smoke, which is different from actual fire and need to be improved further by using new combustion models.

4.2. Comparison of the maximum temperature at 1.8 m high

Figs. 27 and 28 show the maximum temperature at safety height (1.8 m high) of simulation results and experimental data. It can

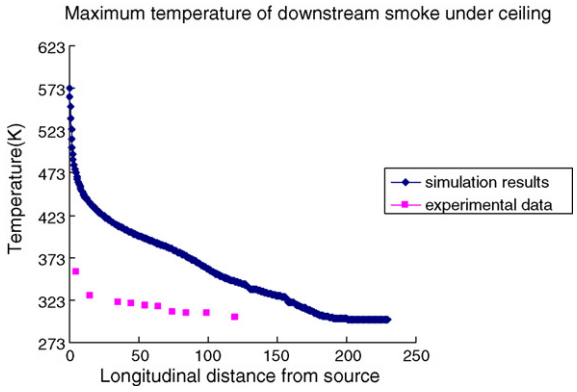

Fig. 26. Maximum temperature under ceiling of different downstream distance from fire source.

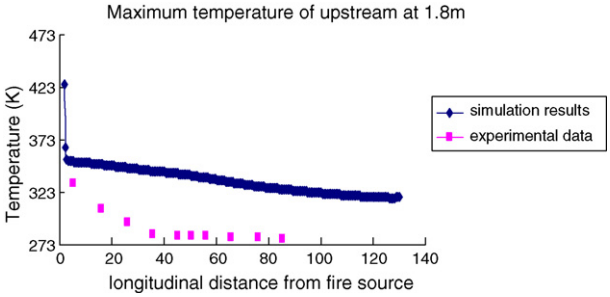

Fig. 27. Maximum temperature of upstream smoke at 1.8 m high.

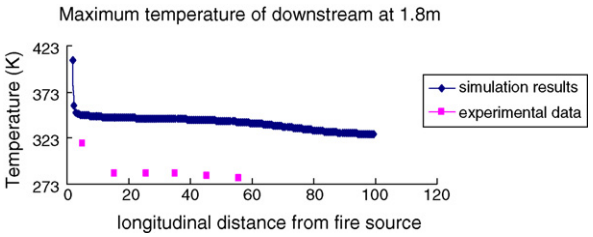

Fig. 28. Maximum temperature of downstream smoke at 1.8 m high.

be seen that the smoke temperatures at safety height is high in the vicinity of the fire source, but it decreases quickly to the ambient temperature, which do not threaten personnel safety. Simulative temperature is much higher than experimental data, which is because the adiabatic boundary conditions are assumed on all the solid walls in simulation. The wall-function method needs to be improved further.

4.3. Comparison of smoke longitudinal propagation

Comparison of smoke longitudinal propagation between simulation results and experimental data are shown in Figs. 29 and 30. From the two figures, we can see that simulation results are identical with experimental data: smoke spreads around 200 m downstream and upstream after 400 s; longitudinal propagation of downstream smoke is quicker than upstream, which is more obvious near the fire source; the smoke longitudinal propagation is slow, which does not affect the personnel evacuation, and there is enough time for evacuating. Hence the roof openings are useful for restraining the longitudinal propagation of smoke.

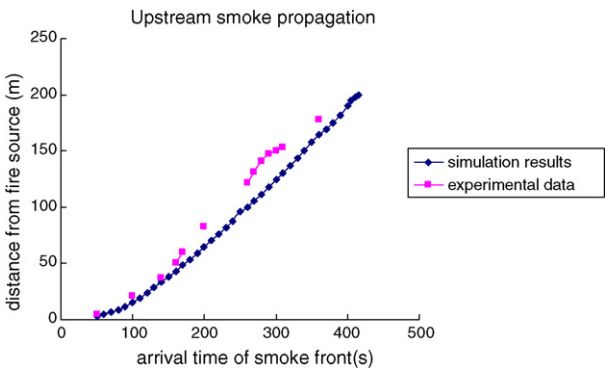

Fig. 29. Upstream smoke propagation.

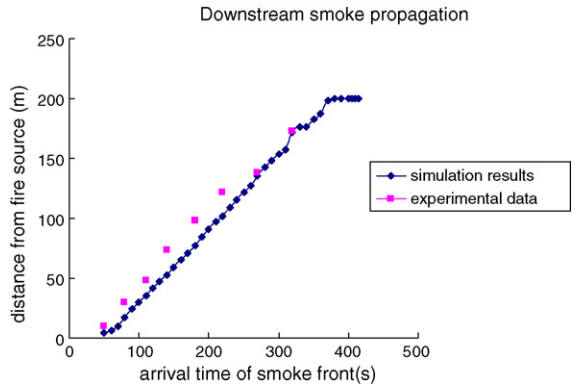

Fig. 30. Downstream smoke propagation.

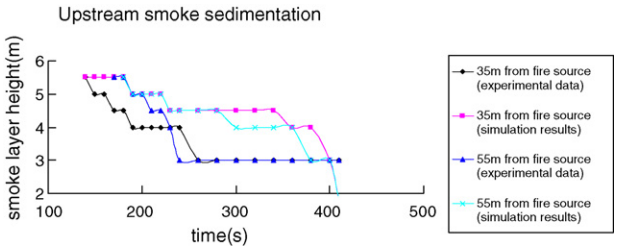

Fig. 31. Upstream smoke sedimentation.

4.4. Comparison of smoke sedimentation

Figs. 31 and 32 plot the smoke sedimentation of simulation results and experimental data, which is analyzed as follows: the difference between simulation results and experimental data is large, which is mainly because it is difficult to judge the height of smoke layer in the experiment. But the whole tendency is similar: the smoke layer in the vicinity of the fire source is higher and lowers gradually far away from fire source; upstream smoke layer is lower than downstream smoke layer. Stratification phenomenon of simulation results is more evident than that in the experiment, which is due to the air agitation of outside wind in the experiment. Smoke downdraught through roof openings is observed from simulation results, which is identical with experimental phenomenon. This downdraught phenomenon may decrease the visibility range and bring panic, so it is necessary to research more efficient ways for improving the smoke removal efficiency, such as early fire detection systems, adequate warning signs and setting funnel cap are required to reduce the risk of being trapped in the smoke plume.

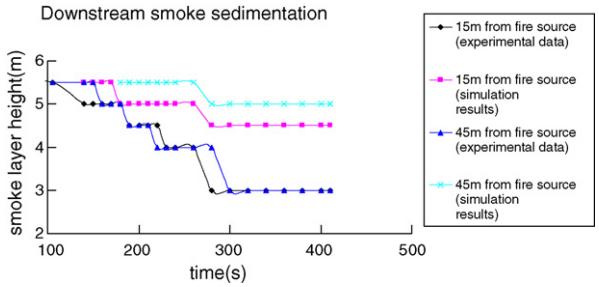

Fig. 32. Downstream smoke sedimentation.

5. Conclusions

From above experimental data and simulation results, it can be achieved that:

(1) In the vicinity of the fire source, temperatures under the ceiling are quite high but temperatures lower continuously with the increase of the longitudinal distance, which does not pose a threat to tunnel structure. The maximum temperatures at 1.8 m high lower rapidly to ambient temperature, which does not threaten personnel safety.
(2) The longitudinal propagation is slow: smoke spreads around 200 m away from fire source after 400 s, which do not affect the personnel evacuation. Smoke layer keeps equilibrium in the early stage but some smoke particle begin to descend about 600 s after ignition, which leads to visibility's falling and difficulty for breath, so evacuee had better evacuate far away from fire source in 600 s.
(3) Most smoke flow out off tunnel through roof openings, so roof openings are favorable for exhausting smoke. But along with the decrease of smoke temperatures, some smoke may back flow and mix with smoke-free air.
(4) The comparisons between simulation results and experimental data show that the built model can be used to predict the tunnel fire with roof openings approximately.

Acknowledgements

This work was supported by National Natural Science Foundation of China under Grant No. 29936110 and 50206009. The experiment introduced in this paper was carried out by Nanjing University of Technology under the cooperation of the Second Survey and Design Institute of China Railway. The authors are indebted to Xingcan Zhong of the Second Survey and Design Institute of China Railway, Jinfeng Mao of PLA University of Science and Technology, Yanfeng Gong, Ru Zhou and members of Heating and Ventilating graduate school, who are a great help in the experiments.

References

[1] R.O. Carvel, A.N. Beard, P.W. Jowitt, The influence of longitudinal ventilation systems on fires in tunnels, Tunn. Undergr. Sp. Tech. 16 (2001) 3–21.
[2] S.R. Lee, H.S. Ryou, A numerical study on smoke movement in longitudinal ventilation tunnel fires for different aspect rate, Build. Environ. 41 (2006) 719–725.
[3] R. Carvel, G. Marlair, A history of experimental tunnel fires, in: The Handbook of Tunnel Fire Safety, Thomas Telford, London, 2005, pp. 201–230.
[4] H. Kurioka, Y. Oka, H. Satoh, O. Sugawa, Fire properties in near field of square fire source with longitudinal ventilation in tunnels, Fire Safety J. 38 (2003) 319–340.
[5] M. Muñoz, E. Planas, F. Ferrero, J. Casal, Predicting the emissive power of hydrocarbon pool fires, J. Hazard. Mater. 144 (2007) 725–729.
[6] Y. Kunikane, N. Kawabata, K. Takekuni, Heat release rate induced by gasoline pool fire in a large-cross-section tunnel, in: Proceedings of the 4th International Conference on Tunnel Fires, Basel, Switzerland, December 2–4, 2002, pp. 387–396.
[7] B. Karlsson, J.G. Quintiere, Enclosure Fire Dynamics, CRC Press LLC, London, 2002.
[8] F. Ferrero, M. Munoz, B. Kozanoglu, J. Casal, J. Arnaldos, Experimental study of thin-layer boilover in large-scale pool fires, J. Hazard. Mater. A137 (2006) 1293–1301.
[9] L.H. Hu, W. Peng, R. Huo, Critical wind velocity for arresting upwind gas and smoke dispersion induced by near-wall fire in a road tunnel, J. Hazard. Mater. 150 (2008) 68–75.
[10] Y.F. Wang, J.C. Jiang, D.Z. Zhu, Full-scale experiment research and theoretical study for fires in tunnels with roof openings, Fire Safety J., (2008), doi:10.1016/j.firesaf.2008.08.001.
[11] J. Abanto, M. Reggio, D. Barrero, E. Petro, Prediction of fire and smoke propagation in an underwater tunnel, Tunn. Undergr. Sp. Technol. 22 (2006) 90–95.
[12] Fluent Inc., Fluent 6.3 User's Guide, Lebanon, NA, 2006.
[13] H. Xue, J.C. Ho, Y.M. Cheng, Comparison of different combustion models in enclosure fire simulation, Fire Safety J. 36 (2001) 37–54.
[14] J. García, E. Migoya, J.A. Lana, A. Crespo, Study of the dispersion of natural gas issuing from compressor stations through silencers with upper cover, J. Hazard. Mater. 152 (2008) 1060–1072.